

1 **Rhizomes play significant roles in biomass accumulation, production and carbon**
2 **turnover in a stand of the tall bamboo *Phyllostachys edulis***

3

4 Keito Kobayashi¹, Mizue Ohashi², Michiro Fujihara³, Kanehiro Kitayama¹, Yusuke

5 Onoda¹

6

7 ¹Graduate School of Agriculture, Kyoto University, Kitashirakawa Oiwake-cho,

8 Sakyo-ku, Kyoto, 606-8502, Japan

9 ²School of Human Science and Environment, University of Hyogo, 1-1-12

10 Shinzaikehoncho, Himeji-city, Hyogo, 670-0092, Japan

11 ³Awaji Landscape Planning and Horticulture Academy/ Graduate School of

12 Landscape Design and Management, University of Hyogo, 954-2 Nojimatokiwa,

13 Awaji-city, Hyogo, Japan

14

15 **Correspondence**

16 Keito Kobayashi,

17 Graduate School of Agriculture, Kyoto University, Kitashirakawa Oiwake-cho, Sakyo-
18 ku, Kyoto, 606-8502, Japan.

19 Email: kobakei1105@ffpri.affrc.go.jp

20

21 Present address

22 Keito Kobayashi,

23 Kansai Research Center, Forestry and Forest Products Research Institute, Kyoto, Japan

24 **ABSTRACT**

25 *Phyllostachys edulis* (Poales: Poaceae) is a bamboo species with well-developed
26 rhizomes, which play important roles in growth, resource storage and transport.
27 However, the extent to which rhizomes are produced, accumulated and turn over
28 annually at the stand level remains largely unknown. We studied the biomass,
29 production and turnover rate of rhizomes and other organs (culms, branches, leaves and
30 roots) in a bamboo stand in Japan **between 2013 and 2018**. We sought to answer the
31 following questions: To what extent is the newly assimilated carbon allocated to
32 rhizomes, and how rapid is carbon turnover in rhizomes? How does biomass allocation
33 to below-ground parts in bamboo ramets compare to that in woody plant individuals **of**
34 **similar size**? We found the amount of newly produced rhizomes was 0.90 Mg C ha⁻¹
35 year⁻¹, which accounted for 9.5% of total new biomass. The carbon turnover rate of
36 rhizomes was 0.11 g g⁻¹ year⁻¹, which was slower than that of other organs (i.e., longer
37 lifespan). Compared **to other woody plants of similar biomass, bamboo had 2.0-fold**
38 **higher biomass allocation to below-ground organs due to the high biomass of**
39 **rhizomes. Furthermore, bamboo allocated 8.7-fold lower biomass to leaves despite their**

40 high growth rates, perhaps due to the thin (but leathery) leaves and green stems that can
41 photosynthesize as well. Our study highlights that the large storage capacity of below-
42 ground rhizomes along with the efficient above-ground production system are the key
43 growth features of *P. edulis*, which are likely to contribute to their success in temperate
44 forest areas.

45

46 **KEYWORDS:** Carbon cycle, biomass allocation, air spade, clonal growth, moso
47 bamboo

48

49 **Introduction**

50 Moso bamboo, *Phyllostachys edulis* (Poales: Poaceae), is a tall temperate bamboo
51 species native to China that forms large clonal colonies (up to 25 m in height). This
52 species has been introduced into many countries, including Japan, because of its high
53 value for the production of food, fibers and building materials (Suzuki 1978). While
54 moso bamboo can be categorized as an herbaceous plant based on the absence of stem
55 secondary growth, it often forms tall stands with similar or greater height than
56 neighboring forests. Therefore, moso bamboo behaves like a tree in terms of its stature
57 and roles in the forest ecosystem (e.g., carbon storage and nutrient cycle). For example,
58 moso bamboo stands can store considerable amounts of carbon, sometimes exceeding
59 100 Mg C ha⁻¹ in East Asia (90% quantile range, 7.5–73.9 Mg C ha⁻¹; Yuen et al.
60 2017); the amounts can exceed those in forests in the same region (e.g., Fukushima et
61 al. 2015; Song et al. 2017). These stands have high productivity (6.5–14.4 Mg C ha⁻¹
62 year⁻¹), comparable to or higher than that of forests in the same region (Lin et al. 2017).
63 This bamboo species as well as other tall bamboo species differ from most woody
64 plants (trees) in terms of its growth strategy; it rarely reproduces sexually and instead is

65 propagated asexually via the production of new shoots from below-ground rhizomes.
66 The new above-ground shoots grow very rapidly, reaching a height of more than 10 m
67 within a few months (e.g., Ueda 1960; Yen 2016); this may be due to large stores of
68 carbon and nutrients in the rhizome system. Therefore, clarifying the ecology and
69 function of bamboo rhizomes, such as their morphological characteristics, mass
70 allocation, and production and turnover rates, could provide novel insights into the
71 success of moso bamboo in temperate forest areas.

72 The morphology and growth characteristics of moso bamboo rhizomes have
73 been investigated over the last half century (e.g., Ueda 1960; Zheng et al. 1998; Kawai
74 et al. 2008; Xiao et al. 2021; Li et al. 2021). Rhizomes, which are typically cylindrical
75 in shape (of diameter ca. 2 cm and each length ca. 1–2 m) with internodes every ca. 4
76 cm, are often concentrated in the top 0.3 m of soil (e.g., Li et al. 1999; Xiao et al. 2021;
77 Li et al. 2021). New rhizomes are produced every year during summer and autumn,
78 branching from the previous year's rhizome fragment (typically at an angle of less than
79 30 degrees; Li et al. 2021). Each node on the rhizome has one lateral bud, and less than
80 1% of buds typically give rise to above-ground shoots (Ueda 1960; Utsunomiya 1976;

81 Nonaka 1987). Rhizomes that are 2–6 years old produce the most shoots (Ueda 1960).
82 In addition to information on their growth characteristics, the total length and mass of
83 rhizomes per ground area have been evaluated both through destructive excavation
84 (e.g., Ueda 1960) and non-destructive technologies such as ground-penetrating radar
85 (e.g., Xiao et al. 2021). Studies on the carbon sink capacity of moso bamboo stands in
86 East Asia showed that rhizome biomass accounts for on average 31% of total biomass at
87 the stand levels (Lin et al. 2017; Yuen et al. 2017). Such high biomass fraction in
88 rhizomes is a key feature of bamboo stands, and could be driven by either the slower
89 turnover (i.e., longer lifespan) of rhizomes or greater allocation of newly produced
90 biomass to rhizomes (i.e., higher rhizome net primary productivity, NPP) compared to
91 other organs especially roots. However, to our knowledge, no such quantitative
92 assessment has been conducted to date.

93 Some previous studies have assumed that below-ground NPP, including
94 rhizome NPP, could be estimated from above-ground NPP under the assumption that
95 the ratio of below- to above-ground NPP is equal to that of below- to above-ground
96 biomass (i.e., the turnover rate is the same for above- and below-ground organs; Suzuki

1976; Tang et al. 2015a, 2015b, 2016; Song et al. 2017; Song et al. 2020); other studies ignored rhizome NPP in the calculation of below-ground NPP (Li et al. 2006; Lin et al. 2017; Shimono et al. 2021). The ratio of below- to above-ground biomass would not be equal to that of below- to above-ground NPP if the carbon turnover rate differs between above- and below-ground organs. As lifespans differ among organs (e.g., a rhizome may have a much longer lifespan than a root), the turnover rate, expressed as the inverse of the lifespan, is expected to also differ among organs. Therefore, below-ground NPP, including rhizome NPP, must be evaluated independently from above-ground NPP. Root NPP has been estimated using an in-growth core method in some studies (Liu et al. 2013; Lin et al. 2017; Shimono et al. 2021), but rhizome NPP has never been estimated in bamboo stands because the rhizomes are too large for the in-growth core method.

The rhizome systems of moso bamboo stands contribute to higher biomass allocation in below-ground parts, as described above. However, these biomass allocation patterns remain unclear at the individual unit level. Moso bamboo stands are comprised of individual bamboos (ramets), each of which can be compared to an

113 individual woody plant. Such comparisons between moso bamboo ramets and woody
114 plant individuals may provide new insight into the growth strategy of moso bamboo. As
115 the biomass allocation pattern varies among organs according to their size (Poorter et al.
116 2015), interspecific differences in biomass allocation may be well evaluated through
117 comparison of individuals of similar size.

118 In the present study, we evaluated biomass accumulation, new production
119 amounts and turnover rates for all organs including rhizomes, roots, culms, branches
120 and leaves in a stand of moso bamboo, *P. edulis*, in the warm temperate zone of Japan.
121 Specifically, we focus on below-ground rhizomes and address the following questions.
122 (1) To what extent is newly assimilated carbon allocated to below-ground organs,
123 particularly rhizomes? (2) How does the carbon turnover rate of rhizomes compare to
124 those of other organs including culms, branches, leaves and roots? (3) To what extent
125 do moso bamboo ramets differ in biomass allocation compared to woody plant
126 individuals when the comparison involves similarly size (i.e., similar stem dry mass)?

127

128

129 **Materials and Methods**

130 *Term definitions*

131 Moso bamboo (*Phyllostachys edulis*; often reported as *P. pubescens*) exhibits clonal
132 growth. An individual unit (ramet) is composed of a culm (= stem), branches and
133 leaves, and the associated rhizomes and roots. A culm consists of above- and below-
134 ground parts (connecting stem between the rhizome and the above-ground culm), and
135 the latter portion is called the "culm base". Note that "below-ground culm base" in the
136 present study was referred to as the "stump" in Fukushima et al. (2015).

137 Biomass at the stand level was expressed as carbon mass in grams. The carbon
138 concentration in each organ was taken from Fukushima et al. (2015), with consideration
139 of the age class of culms (see Table S1). Below-ground organs including rhizomes and
140 roots cannot be readily divided into each ramet due to their complex structures (see
141 example in Figure 1b). Here, the average below-ground biomass per ramet was
142 estimated from the ground area occupied by each culm, which was determined from the
143 spatial distribution of above-ground culms, as described below. While the below-ground
144 culm base is part of the culm in terms of morphology, it was included in below-ground

145 biomass in our analysis of the biomass distribution using above- and below-ground part
146 categories.

147 NPP can be defined as the sum of the net increase in biomass, litter production, and
148 biomass losses obtained through herbivory over a given period (e.g., Ogawa 1977). A
149 bamboo stand consists of culms, branches, leaves, roots and rhizomes; therefore, NPP
150 can be calculated separately for each organ (e.g., Isagi et al. 1997). In general, biomass
151 loss due to herbivory is quite small, and is thus ignored in the calculation of NPP (Isagi
152 et al. 1997; Lin et al. 2017). While culms do not undergo secondary growth, the mass of
153 culms increases slightly with age (e.g., the mass of one-year culm is three-fourths that
154 of a five-year-old culm; Yen and Lee 2011; Yen 2016). We calculated the NPP of
155 above-ground culms from the amount of newly produced culms considering the
156 biomass increment with culm age, as described below. NPPs of branches, rhizomes and
157 below-ground culm bases were calculated from the amounts of newly produced
158 branches, rhizomes and below-ground culm bases, respectively. Leaves were renewed
159 during the census period even within a culm, so we estimated the NPP of leaves from
160 the standing leaf mass considering leaf longevity, as described below. Root NPP was

161 calculated as the increase in living root biomass considering the mass balance between
162 living and dead root biomass (Fairley and Alexander 1985; Brunner et al. 2013). Other
163 minor tissues, including sheaths, twigs and undeveloped sprouts, are also produced in
164 moso bamboo stands, but were excluded from the estimation of NPPs because they
165 account for negligible biomass compared to the stand as a whole (e.g., Goto et al. 2008).

166

167 *Site description and plot establishment*

168 The present study was conducted in a moso bamboo stand on Awaji Island, Hyogo
169 Prefecture, western Japan (34°33'43.2"N 134°57'54.7"E, 250 m above sea level) (Figure
170 1a). This bamboo stand has existed for more than 40 years, as confirmed by aerial
171 photographs taken by local governments in 1975, and has been selectively logged by the
172 landowners once or twice per year, without fertilization, until the present study began in
173 2013. The average culm size was 7.6 cm in diameter at breast height (DBH) and 11 m in
174 height from the ground. The density of living culms was 7,600 culms ha⁻¹. This bamboo
175 stand grows on a gentle slope facing southward (16.5° on average). The mean annual air
176 temperature (MAT) and mean annual precipitation (MAP) were 15.9°C and 1,167 mm,

177 respectively at Gunge, which is the nearest meteorological station, located 15 km from
178 the study site (average values between 1976 and 2019). Understory vegetation was
179 sparse (Figure 1a), comprising only a few small plants such as *Camellia japonica*. The
180 soil type is categorized as clay loam derived from rhyolite.

181

182 ***Biomass and NPP of above-ground organs***

183 In September 2013, three 8 m × 8 m plots were established, which were placed ca. 2 m
184 apart within the study stand (Figure 1a). The culm DBH, living status (alive or dead)
185 and location of each culm in the three plots were recorded every autumn or winter for 5
186 years, 2013 to 2017. As moso bamboo stands typically exhibit a biennial growth pattern
187 (Li et al. 1998a, see Table S3), more than two years of study are needed for estimation
188 of mean biomass and NPP. The biomass of above-ground organs was estimated from
189 culm DBH using the following allometric equations, with one-year culms and those
190 older than one year (according to previous studies in Japan; e.g., Isagi et al. 1997; Abe
191 and Shibata 2009; Fukushima et al. 2015) considered separately:

192 $M_{ij} = \alpha DBH^\beta$ (1)

193 where M is biomass; DBH is culm diameter at breast height; i is the organ (culms,
194 branches or leaves); j is culm age class (one or more than one year old); and α and β are
195 constants. We employed two allometric equations, i.e., those of Kaku et al. (2014) and
196 Abe and Shibata (2009) (Table S2). The allometric equation of Kaku et al. (2014) was
197 obtained at a site very close to our study site, but was applicable only to culm biomass
198 for culms older than one year. Abe and Shibata (2009) reported more comprehensive
199 allometric equations with consideration of culm age class and multiple organs, but their
200 study site was remote from ours. Here, we used a combined approach. First, we
201 calculated the difference in estimated biomass between the two equations for culms
202 older than one year. The ratio of these two values (calculated biomass ratio, R_{culm}) can
203 be expressed as follows:

204 $R_{culm} = \frac{M_{c1}}{M_{c2}} = \frac{9.7 \times 10^{-2} DBH^{2.049}}{1.305 \times 10^{-1} DBH^{2.052}} = 7.4 \times 10^{-1} DBH^{-0.003}$ (2)

205 where M_{c1} represents culm biomass for bamboo culms older than one year estimated
206 with the method of Kaku et al. (2014), and M_{c2} is the corresponding value estimated

207 with the equation of Abe and Shibata (2009). As the estimated culm biomass based on
208 Kaku et al. (2014) was lower than that based on Abe and Shibata (2009) (see equation
209 2), the biomass of culms, branches and leaves in both age classes was estimated using
210 the equations of Abe and Shibata (2009) with adjustment based on R_{culm} , as follows:

$$211 \quad M_{ij} = \alpha DBH^{\beta} R_{culm} \quad (3)$$

212 The culm, branch and leaf biomass of each living bamboo were summed for
213 each plot, expressed per unit ground area (g m^{-2}), and converted into total above-ground
214 biomass (Mg C ha^{-1}). As the biomass of the below-ground culm base was not
215 considered in the equations above, we considered this biomass separately using an
216 allometric equation reported by Fukushima et al. (2015) (see Table S2), with adjustment
217 based on R_{culm} shown in equation 2. Biomass was calculated for each year in the period
218 2013–2017, and average values over five years were used for further analysis.

219 The NPP of culms, including below-ground culm bases (culm NPP, Mg C ha^{-1}
220 year^{-1}), and branches (branch NPP, $\text{Mg C ha}^{-1} \text{ year}^{-1}$) was calculated from the culm
221 DBH of newly produced culms in each plot over five years from 2013 to 2017; the

222 average values over five years were used for further analysis. As noted above, above-
223 ground culms accumulate three-fourths of their biomass in the first year and then
224 accumulate slowly (Yen and Lee 2011). Thus, above-ground culm NPP originating
225 from newly emerged culms was calculated using allometric equations for one year in
226 the first year, and the biomass increment was then added in the second year (i.e., the
227 difference between the biomass of culms older than one year and one-year). The leaf
228 lifespan of moso bamboo is typically two years, except in one-year culms, where its
229 lifespan is only one year (Li et al. 1998a). Considering the leaf lifespan of moso
230 bamboo, the NPP of leaves (leaf NPP, Mg C ha⁻¹ year⁻¹) can be calculated as the sum of
231 newly produced leaf biomass originating from one-year culms and a half of the leaf
232 biomass originating from culms older than one year. We estimated leaf NPP for each
233 plot based on culm data for five years from 2013 to 2017, and the average values were
234 used for further analysis.

235

236 *Biomass and NPP of roots*

237 The biomass and NPP of roots (root NPP, $\text{g C m}^{-2} \text{ year}^{-1}$) were estimated using an in-
238 growth core technique (e.g., Brunner et al. 2013). In December 2013, 12 cylindrical
239 mesh bags, 55 mm in diameter, 0.3 m in length and with a $5 \text{ mm} \times 5 \text{ mm}$ mesh size,
240 were filled with root-free soil and buried around each of the three plots (36 in-growth
241 cores in total). After 12 and 24 months, six in-growth cores per plot were collected
242 (total of 18 in-growth cores per sampling time). For each core, the living and dead roots
243 were separated, by hand and with tweezers, based on their texture and color (Vogt and
244 Persson 1991). Roots were then oven-dried at 70°C for two days, and their dry weight
245 was determined with a digital balance. Root NPP ($\text{g C m}^{-2} \text{ year}^{-1}$) was calculated from
246 the difference between living and dead root biomasses, as well as the measurement
247 interval, according to the decision matrix method described by Fairley and Alexander
248 (1985). As root biomass was not measured before installing in-growth cores, it was
249 measured in the same plot and manner in December 2019 as in December 2013.

250

251 ***Morphological characteristics, biomass and NPP of rhizomes***

252 To measure rhizome morphology and estimate biomass, the surface soil was removed to
253 a depth of 0.5 m with an air spade (screw compressor: PDS130S; Hokuetsu Industries
254 Co. Ltd., Niigata, Japan) in April 2014 (Figure 1b). As the excavation survey was very
255 laborious and caused relatively major disturbance to the plot, we established only two 2
256 m × 2 m subplots, in two of the three plots. Each subplot was subdivided into 16 0.5 m
257 × 0.5 m sub-subplots (see Figure S1). Soil was removed in two steps due to the high
258 density of roots; the first excavation typically reached 0–0.2 m in depth and the second
259 was to a depth of 0.5 m. The second excavation was conducted after all roots in the 0.2-
260 m layer had been carefully collected for biomass measurement. Despite collecting as
261 many roots as possible, the root biomass measured in this manner was underestimated
262 by 48% compared to measurements obtained with the soil core sampling method. All
263 rhizomes in each sub-subplot were labeled, and their diameters **in two orthogonal**
264 **directions at both ends**, length, number of nodes and deepest and shallowest distances
265 from the surface were measured. We constructed a distribution map of rhizomes for
266 each sub-subplot. The excavated areas were refilled with their original soils and covered
267 with surface litter in May 2014 after sampling and measurement. During the period of

268 excavation (ca. 1 month), the excavated rhizome systems were covered with
269 polyethylene sheets and watered regularly to avoid drying.

270 The volume of a rhizome can be calculated from its diameter and length by
271 assuming a cylindrical shape (e.g., Xiao et al. 2021).

$$272 \quad V_s = \frac{\pi D_s^2 L_s}{4} \quad (4)$$

273 where V_s is the estimated volume of rhizomes (cm^3), and D_s and L_s are the diameter and
274 length of rhizomes (cm) in the sub-subplot. The total estimated volume (cm^3) of
275 rhizomes in each sub-subplot was calculated as the sum of V_s for all rhizomes in each
276 sub-subplot. To convert the volume of these rhizomes into biomass, we estimated
277 rhizome tissue density (d , g cm^{-3}) for a subset of rhizomes collected randomly from 15
278 sub-subplots. Tissue density was calculated as the dry mass of a rhizome divided by its
279 fresh volume. The sampled rhizomes were washed, wiped dry with towels, oven-dried
280 at 70°C for at least five days until the weight became constant, and then weighed with a
281 digital balance. The average rhizome tissue density (d) was 0.61 g cm^{-3} , and this value
282 was used to convert volume into biomass for rhizomes (g C m^{-2}).

283 The standard in-growth core method cannot be used to measure rhizome NPP,
284 because the size of the core (approximately 5 cm in diameter) is typically too small for
285 rhizomes to penetrate. Therefore, we applied the concept of the in-growth core at a
286 larger scale by repeatedly excavating the same ground area with a four-year time
287 interval to estimate rhizome NPP. In April 2018, we removed the surface litter and soil
288 to a depth of 0.5 m, in the same location and manner as in 2014. First, we confirmed
289 that remaining rhizomes found in 2014 were all dead (but their debris existed); second,
290 we observed that all new rhizomes were living (no turnover of new rhizomes within 4
291 years). All new rhizomes in each sub-subplot were then labeled and their diameter (in
292 the orthogonal direction), length, number of nodes and deepest and shallowest distances
293 from the ground surface were measured (Table S4). The total biomass of new rhizomes
294 in each sub-subplot was estimated through the method described above. We calculated
295 NPP of rhizomes as the biomass of new rhizomes divided by the time interval (four
296 years) (rhizome NPP, $\text{g C m}^{-2} \text{ year}^{-1}$), as no new turnover observed within this period.

297

298 ***Data analysis***

299 All data analyses were conducted with the *R* statistical package (version 4.1.2; *R* Core
300 Team 2021). Data from two subplots for rhizome variables and three plots for root
301 measurements were pooled for analysis. The turnover rate was calculated as biomass
302 divided by NPP, and this calculation was conducted for each organ. We evaluated the
303 relative variation (coefficient of variation [CV] = standard deviation per mean) of the
304 measured below-ground data (morphology, biomass and NPP) in plots of various sizes
305 (0.25, 1.0 and 4.0 m²), as horizontal heterogeneity is high for these data and few studies
306 have considered the effect of plot size in below-ground surveys (causing major
307 uncertainty in below-ground data for bamboos; Zhang et al. 2005; Yuen et al. 2017).
308 We analyzed CV sensitivity according to plot size among below-ground variables.

309 Below-ground biomass in each plot was partitioned into bamboo culms under
310 the assumption that the relative proportions of below-ground biomass attributed to
311 bamboo ramets were equal to the relative proportions of space occupancy by those
312 ramets, determined using Voronoi partitioning based on the locations of culms (Li et al.
313 1998b; see Figure 1c). Each plot was divided into multiple tiles based on culm location
314 through a Dirichlet tessellation method, using the *voronoi mosaic* function in *R*. Only

315 closed tiles were used; edge data were excluded from the analysis (Table S7). The
316 locations of culms in 2017 were used for analysis. Note that the below-ground biomass
317 was calculated from the rhizome biomass measured in 2014 and root biomass in 2019.

318

319

320 **Results**

321 *Rhizome characteristics*

322 The morphological characteristics of rhizomes in the study stand are summarized in
323 Table 1 and Table S5. Rhizomes spread extensively in the horizontal direction, with an
324 average rhizome diameter of 21 mm. The total length of rhizomes averaged 8.4 m, with
325 230 nodes per unit square meter. The vertical distribution typically ranged between 0
326 and 0.2 m in depth and rhizomes were scarce below 0.4 m (Figure S3).

327

328 *Biomass accumulation*

329 The total biomass of the study stand averaged 46 Mg C ha⁻¹ and the biomass fractions
330 of culms, branches, leaves, rhizomes and roots were 26 ± 8.7, 2.5 ± 0.70, 0.65 ± 0.16,

331 8.1 ± 4.5 and 8.4 ± 2.8 Mg C ha⁻¹, respectively (mean \pm standard deviation) (Figure
332 2a). Rhizomes were the third largest component among these organs, accounting for
333 18% of the total biomass. Among below-ground parts, rhizome biomass was 0.96 times
334 the root biomass and 2.3 times the below-ground culm base biomass, accounting for
335 41% of total below-ground biomass (Table 1; Figure 2a; Figure S6). The ratio of below-
336 ground biomass (rhizomes + roots + below-ground culm bases) to above-ground
337 biomass (above-ground culms + branches + leaves) was 0.80.

338

339 *NPP and turnover rate*

340 The annual NPP of the study stand during the study period averaged 9.5 Mg C ha⁻¹
341 year⁻¹. At the organ level, the NPP values for culms, branches, leaves, rhizomes and
342 roots were 4.6 ± 1.6 , 0.53 ± 0.20 , 0.41 ± 0.13 , 0.90 ± 0.76 and 3.1 ± 2.4 Mg C ha⁻¹ year⁻¹,
343 respectively (Figure 2b; Table S3). Rhizomes were the third largest component,
344 accounting for 9.5% of the total NPP. Among below-ground parts, rhizome NPP
345 was 0.29 times the root NPP and 1.4 times the culm base NPP, accounting for 19% of

346 total below-ground NPP (Table 1; Figure 2b; Table S3). The ratio of below- to above-
347 ground NPP was 0.94, which differed from the ratio of biomass described above (0.80).

348 The turnover rate of the study stand averaged $0.21 \text{ g g}^{-1} \text{ year}^{-1}$. The turnover rate
349 averaged 0.18, 0.21, 0.63, 0.38 and $0.11 \text{ g g}^{-1} \text{ year}^{-1}$ for culms, branches, leaves,
350 rhizomes, and roots, respectively (Figure 2c). The turnover rate of rhizomes was lowest
351 among all organs.

352

353 ***Biomass allocation pattern within individual units***

354 In Figure 3, we show the biomass (not carbon mass) allocations among organs at the
355 individual level in our studied bamboo and woody plants that was compiled by Poorter
356 et al. (2015). As biomass was subdivided into *leaves*, *stems* and *roots* in the dataset of
357 Poorter et al. (2015), the biomass of our studied moso bamboo ramets was subdivided
358 into the same categories, i.e., *leaves*, *stems* (above-ground culms + branches) and *roots*
359 (roots + rhizomes + below-ground culm bases) for this comparison ($n = 86$). In addition,
360 this comparison was made for woody plants with *stem* biomass ranging from 0.66 to 14
361 kg ($n = 842$), which is equivalent to the range of moso bamboo ramets in the present

362 study. Biomass allocation to *stems* tended to be similar between moso bamboo ramets
363 (0.54 ± 0.13 , mean \pm standard deviation) and woody plant individuals (0.65 ± 0.10).
364 Biomass allocation to *roots*, i.e., below-ground organs, was much higher in moso
365 bamboo (0.44 ± 0.13) than woody plants (0.22 ± 0.083), while biomass allocation to
366 *leaves* was much lower in moso bamboo (0.015 ± 0.0037) than woody plants ($0.13 \pm$
367 0.082).

368

369 *Spatial heterogeneity of below-ground data according to plot size*

370 The plot-size dependency of the below-ground traits was evaluated by plotting the CV
371 against plot size (Figure 4). CV decreased with increasing plot size for all variables.
372 Because rhizomes are much larger structures than roots, rhizome biomass showed a
373 higher CV than root biomass, especially at smaller plot sizes (Figure 4d, f). This
374 increased variation of rhizome biomass was due to greater variation in rhizome length
375 (and consequently node numbers) per unit ground area (Figure 4c), and not to variation
376 in rhizome diameter (Figure 4b).

377

378

379 **Discussion**

380 In the present study, we evaluated the biomass accumulation, NPP and carbon turnover
381 rate for each organ, namely culms, branches, leaves, roots and rhizomes, in a stand of
382 moso bamboo, *Phyllostachys edulis*. We found that below-ground rhizome production,
383 which has never been quantified (Shimono et al. 2021), played significant roles within a
384 moso bamboo stand due to the longer lifespan of rhizomes. We also found that biomass
385 allocation to leaves was quite low in moso bamboo ramets despite their high NPP,
386 which may be another unique characteristic of this bamboo. In the following sections,
387 we first discuss biomass accumulation and NPP in our study stand. Second, we discuss
388 NPP and turnover rates of rhizomes to address questions (1) and (2). Third, we discuss
389 unique biomass allocation patterns within moso bamboo ramets to address question (3).

390

391 ***Biomass accumulation in the study stand***

392 The biomass of our studied moso bamboo stand averaged 46 Mg C ha⁻¹, which is
393 similar to the mean biomass of other moso bamboo stands in East Asia (46.0 ± 39.8 Mg

394 C ha⁻¹, N = 125 (mean ± standard deviation), Yuen et al. 2017; Lin et al. 2017), but
395 tends to be lower than that of stands in Japan (63.3 ± 31.7 Mg C ha⁻¹, N = 12, Table S6).
396 In Table S6, we summarize existing data on the above- and below-biomass of moso
397 bamboo stands in Japan. Compared to other bamboo stands in Japan, our study stand
398 tended to have higher culm density (7,600 vs. 6,785 ± 2,983 culms ha⁻¹), but lower
399 DBH of individual culms (7.6 vs. 8.7 ± 2.1 cm). The relatively small culm size in our
400 study stand was likely due to local environmental factors including wind, soil
401 conditions (Numata 1962). The relatively short period of time after the stand have been
402 abandoned and have naturalized may also be related. Our study stand was selectively
403 managed until the start of the present study, and then abandoned; therefore, biomass
404 accumulation might have been suppressed to some extent. This possibility is supported
405 by the fact that both culm density and above-ground biomass tended to increase
406 monotonically from 2013 to 2016 (Figure S2a, d).

407 The ratio of below- to above-ground biomass in our study stand was 0.80,
408 which was within the range of previously reported values, although those values varied
409 greatly among study sites and regions (0.55 reported in East Asia by Yuen et al. 2017

410 vs. 0.95 ± 0.56 in Japan, see Table S6). Despite the variation among previous studies,
411 the ratios for bamboo stands, including our study stand, are typically higher than those
412 for temperate forest vegetation (e.g., 0.26 ± 0.07 , $n = 73$, Cairns et al. 1997).

413

414 *NPP in the study stand*

415 The estimated NPP of the study stand, including both above- and below-ground organs,
416 averaged $9.5 \text{ Mg C ha}^{-1} \text{ year}^{-1}$, which is within the range of previous studies but lower
417 than the mean value for moso bamboo stands in East Asia ($6.5\text{--}14.4 \text{ Mg C ha}^{-1} \text{ year}^{-1}$, n
418 $= 10$, Lin et al. 2017). In Japan, the NPP of moso bamboo stands has been estimated in
419 at least four studies. Suzuki (1976) reported ca. $7.3\text{--}11.0 \text{ Mg C ha}^{-1} \text{ year}^{-1}$ ($n = 3$) from
420 four-year surveys conducted in the Kyoto area, and Shimono et al. (2021) reported ca.
421 $6.5\text{--}9.2 \text{ Mg C ha}^{-1} \text{ year}^{-1}$ ($n = 5$) from three-year surveys in Fukuoka Prefecture,
422 respectively. Kawahara et al. (1987) and Isagi et al. (1997) reported ca. $8\text{--}9 \text{ Mg C ha}^{-1}$
423 year^{-1} for above-ground parts from five-year surveys in the same region of the Kyoto
424 area. As above-ground NPP was $4.9 \text{ Mg C ha}^{-1} \text{ year}^{-1}$ in the present study, NPP in this
425 study was lower than the values reported by Kawahara et al. (1987) and Isagi et al.

426 (1997), but similar to that of Suzuki (1976), likely due to differences among local
427 conditions, as described above. As the number of studies that evaluate NPP of bamboo
428 stands remains limited compared to biomass studies, and there is no NPP evaluation to
429 include rhizome data, our results are important for explaining carbon flow in bamboo
430 stands in this region.

431

432 *NPP and carbon turnover rate of rhizomes*

433 We found that the NPP and carbon turnover rate of rhizomes averaged $0.90 \text{ Mg C ha}^{-1}$
434 year^{-1} and 0.11 year^{-1} , respectively, in the stand (Figure 2b, c). The pattern of NPP
435 among organs was similar to that of biomass, except for below-ground parts (Figure 2a,
436 b). NPP was much lower in rhizomes than roots (0.29-fold), while biomass was similar
437 between rhizomes and roots (0.96-fold, Table 1; Figure 2a, b). Roots had higher
438 turnover rates than rhizomes (Figure 2c), probably due to their metabolic activities, such
439 as absorption of nutrients and water, resulting in a much higher NPP for a given
440 biomass of roots. The turnover rate of rhizomes (0.11 year^{-1} , Figure 2c), suggesting a
441 rhizome lifespan of ca. 9–10-years, was consistent with previous findings (rhizomes

442 survived for around 10 years, Ueda 1960). The longer lifespan of rhizomes compared to
443 the other studied organs may be due to their stiff structure and low exposure to
444 disturbances such as strong winds compared to above-ground organs. In terms of the C
445 cycle in bamboo stands, a longer lifespan of rhizomes means that a moso bamboo stand
446 can store and transport resources in below-ground parts for a long time, supporting
447 rapid growth of above-ground shoots.

448 If we calculate below-ground NPP under the assumption that the turnover rate
449 is equal between above- and below-ground organs (i.e., 0.20), as was the case in
450 previous studies (Suzuki 1976; Li et al. 1999; Tang et al. 2015a, 2015b, 2016; Song et
451 al. 2017; Song et al. 2020), below-ground NPP would be 4.0 Mg C ha⁻¹ year⁻¹, which is
452 87% of our result based on direct estimation (4.6 Mg C ha⁻¹ year⁻¹). This study
453 highlights the importance of considering the different turnover rates of each organ for
454 better NPP estimate (Figure 2c), and verifies the accuracy of the previously used
455 method. Nonetheless, our estimates should be considered an initial attempt at
456 elucidating below-ground C dynamics. Some technical challenges in data collection
457 remain, such as the repeated excavations used in the present study, which can damage

458 below-ground organs and cause over- or underestimation of rhizome NPP (a similar
459 argument has been made for the in-growth core method for root NPP; e.g., Hendricks et
460 al. 2006). In addition, management history may have affected our results, as the
461 turnover rate of culms in the present study (0.18, Figure 2c) was higher than expected
462 (typically 0.05–0.1, equating to culm longevity of 10–20 years). Note that the biomass
463 accumulation and NPP of roots and culms might be over- or underestimated, as some
464 roots attached to below-ground culm bases were included in the culm biomass and NPP
465 estimates in the present study. Non-destructive techniques, such as ground penetrating
466 radar, have been used in recent years for rhizome detection in bamboo stands (Xiao et
467 al. 2021), and may constitute a more useful method for estimating rhizome NPP in the
468 future.

469

470 ***Biomass allocation pattern within individual units***

471 Compared to woody plant individuals of similar stem size, our studied moso bamboo
472 ramets had higher average biomass allocation to below-ground parts (44% vs. 22%; 2.0-
473 fold higher than the level in woody plants) and much lower average allocation to leaves

474 (1.5% vs. 13%; 8.7-fold lower than the level in woody plants) (Figure 3). These results
475 suggest that moso bamboo ramets allocate more biomass to below-ground organs
476 compared to woody plants of similar size. Higher biomass allocation to below-ground
477 organs in moso bamboo was partly explained by the large amount of rhizomes, which
478 formed a dense network structure (average = 8.4 m m⁻², see Table 1; Figure 1b; Table
479 S5) because rhizomes are typically not present in woody plants and rhizome biomass
480 comprised 41% of the total below-ground biomass in moso bamboo (Table S6). On the
481 other hand, the average leaf fraction was surprisingly low in moso bamboo (1.5%)
482 compared to woody plant individuals (13%). This low allocation to leaves is consistent
483 with previous studies (e.g., 3–4% of above-ground organs in Yen and Lee 2011, 1–2%
484 in Yen 2016 and 1–6% in Murakami et al. 2006), but its possible mechanism has never
485 been discussed. We proposed the low allocation to leaves may be partly related to its
486 thin leaves. Leaf mass per area of moso bamboo is typically 50–70 g m⁻² (e.g., 61.3 g m⁻²
487 in Li et al. 1999 and 52.8 g m⁻² in Sun et al. 2017), which is typically lower than most
488 tree leaves (Mean ± standard deviation = 122 ± 86.6 (n = 967), Wright et al. 2004). The
489 leaves of moso bamboo are leathery and typically survive for two years (Li et al. 1998a;

490 Itou et al. 2018), possibly due to high Si accumulation (4–7%, Ueda 1960; Umemura
491 and Takenaka 2014). Silica accumulation is considered an adaptive strategy for
492 increasing leaf mechanical strength with minimal C cost, and for reducing biomass
493 investment in leaves (Cooke and Leishman 2011). Another possible explanation for the
494 lower allocation to leaves is that green branches and culms (Figure 1a) may play the
495 role of photosynthetic organs in moso bamboo (as discussed in the following section),
496 which can offset mass allocation to leaves.

497 Despite the low allocation to photosynthesizing leaves and high allocation to
498 below-ground organs, moso bamboo achieve a high growth rate. We propose three
499 possible explanations for this trend. First, the leaves of moso bamboo are evergreen and
500 have higher nitrogen content than those of woody plants (e.g., Fukushima et al. 2015;
501 Song et al. 2017); this may enable moso bamboo to achieve a high photosynthetic rate
502 throughout the year. Second, moso bamboo can photosynthesize through their green
503 branches and culms (Figure 1a), as described above. Chloroplasts in the culms are
504 mainly distributed in chlorenchyma cells under the epidermis, and in cells around the
505 vascular bundle, similar to the Kranz anatomy observed in C4 plants (Wang et al. 2012).

506 High activity of a photosynthetic enzyme, phosphoenolpyruvate carboxylase (PEPC),
507 has been detected in culms, suggesting that an efficient photosynthetic pathway might
508 exist in the culms (Wang et al. 2012). CO₂ released by respiration may partially reused
509 for photosynthesis. However, the extent to which stem/branch photosynthesis
510 contributes to overall photosynthesis remains largely unclear. Third, several
511 characteristics, including efficient height acquisition due to its hollow structure (i.e.,
512 plants are taller per unit biomass), efficient foliage arrangement within the crown that
513 utilizes light efficiently (Li et al. 1999), higher nitrogen use efficiency (Song et al.
514 2017), and high fine root activity (Liu et al. 2013), may contribute to the high
515 productivity of moso bamboo.

516

517 **Acknowledgments**

518 We greatly thank A. Takamatsu and C. Ohnishi for assistance with the field and
519 laboratory work, and K. Miyata and K. Inaba for assistance with the excavation of soils
520 using the air spade. We thank Hyogo Prefectural Awaji Landscape Planning and
521 Horticulture academy (University of Hyogo Awaji campus), and in particular Dr. Y.

522 Sawada, for granting permission to conduct this research on their managed land. Drs.

523 M. Umemura and S. Wang helped us with the literature search.

524

525 **Disclosure statement**

526 The authors declare that this research was conducted in the absence of any commercial

527 or financial relationships that could be construed as potential conflicts of interest.

528

529 **Funding**

530 This study was supported in part by the Sasagawa Scientific Research Grant from The

531 Japan Science Society (No. 2018–5001) and a grant from JSPS KAKENHI (No.

532 19J11336).

533

534 **References**

535 Abe Y, Shibata S. 2009. Stand structure of non-management *Phyllostachys pubescens*
536 forest and dynamics for 3 years after improvement management in Mt. Tennozsan. *J*
537 *Jpn Soc Reveget Tech.* 35:57–62. Japanese with English summary.

- 538 Brunner I, Bakker MR, Björk RG, Hirano Y, Lukac M, Aranda X, Børja I, Eldhuset
539 TD, Helmisaari HS, Jourdan C. 2013. Fine-root turnover rates of European forests
540 revisited: An analysis of data from sequential coring and ingrowth cores. *Plant Soil*.
541 362:357–372.
- 542 Cairns MA, Brown S, Helmer EH, Baumgardner GA. 1997. Root biomass allocation in
543 the world's upland forests. *Oecologia*. 111:1–11.
- 544 Cooke J, Leishman MR. 2011. Silicon concentration and leaf longevity: Is silicon a
545 player in the leaf dry mass spectrum? *Funct Ecol*. 25:1181–1188.
- 546 Fairley RI, Alexander IJ. 1985. Methods of calculating fine root production in forests.
547 In: Fitter AH, Atkinson D, Read DJ, editors. *Ecological interactions in soil: plants,*
548 *microbes and animals*. Oxford: Blackwell; p. 37–42.
- 549 Fukushima K, Usui N, Ogawa R, Tokuchi N. 2015. Impacts of moso bamboo
550 (*Phyllostachys pubescens*) invasion on dry matter and carbon and nitrogen stocks in a
551 broad-leaved secondary forest located in Kyoto, western Japan. *Plant Species Biol*.
552 30:81–95.
- 553 Goto S, Kawai H, Zhang F, Jia S, Saijoh Y, Akiyama T. 2008. Estimation of biomass
554 and carbon storage in abandoned bamboo stands ecosystem. *J Jpn Agric System Soc*.
555 24:243–252. Japanese with English summary.
- 556 Hendricks JJ, Hendrick RL, Wilson CA, Mitchell RJ, Pecot SD, Guo D. 2006.
557 Assessing the patterns and controls of fine root dynamics: An empirical test and
558 methodological review. *J Ecol*. 94:40–57.
- 559 Isagi Y, Kawahara T, Kamo K, Ito H. 1997. Net production and carbon cycling in a
560 bamboo *Phyllostachys pubescens* stand. *Plant Ecol*. 130:41–52.
- 561 Ito T, Yamada M. 2005. Actual condition of bamboo forests and characteristics of the
562 growth of moso bamboo (*Phyllostachys heterocycle* (Carr.) Mitf.). *Bull Agr Food*
563 *Env Res Ctr Osaka*. 41:11–18. Japanese with English summary.

- 564 Itou T, Okuda S, Sakai A. 2018. Inter-annual variations in leaf fall and leaf recovery
565 process in an unmanaged moso bamboo (*Phyllostachys pubescens*) forest after strip
566 cutting: 10 years of observation at the Kochi Prefecture. *J Jpn For Soc.* 100:124–128.
567 Japanese with English summary.
- 568 Kaku M, Fujihara M, Oyabu T, Sawada Y, Yamamoto S. 2014. Possibility of
569 sustainable use of column for fuel and management of bamboo forests on the basis of
570 the estimation of weight and volume of bamboo column in Awaji Island. *Pap*
571 *Environ Inf Sci.* 28:19–24. Japanese with English summary.
- 572 Kawahara T, Kamo K, Isagi Y. 1987. Process of reproduction in the cutting stand of
573 *Phyllostachys pubescens*. *Bamboo J.* 5:63–74. Japanese.
- 574 Kawai H, Saijoh Y, Akiyama T, Zhang F. 2008. The annual rhizome elongation and its
575 growth pattern in *Phyllostachys pubescens*. *J Jpn For Soc.* 90:151–157. Japanese
576 with English summary.
- 577 Kawai H, Saijoh Y, Akiyama T. 2010. Analysis of bamboo stand expansion from the
578 viewpoint of above- and belowground growth. *J Jpn For Soc.* 92:93–99. Japanese
579 with English summary.
- 580 Li R, Werger MJA, During H, Zhong ZC. 1998a. Biennial variation in production of
581 new shoots in groves of the giant bamboo *Phyllostachys pubescens* in Sichuan,
582 China. *Plant Ecol.* 135:103–112.
- 583 Li R, During HJ, Werger MJA, Zhong ZC. 1998b. Positioning of new shoots relative to
584 adult shoots in groves of giant bamboo, *Phyllostachys pubescens*. *Flora.* 193:315–
585 321.
- 586 Li R, Werger MJA, During H, Zhong ZC. 1999. Biomass distribution in a grove of the
587 giant bamboo *Phyllostachys pubescens* in Chongqing, China. *Flora.* 194:89–96.
- 588 Li ZJ, Lin P, He JY, Yang ZW, Lin YM. 2006. Silicon's organic pool and biological
589 cycle in moso bamboo community of Wuyishan Biosphere Reserve. *J Zhejiang Univ*
590 *Sci B.* 7:849–857.

- 591 Li C, Cai Y, Xiao L, Gao X, Shi Y, Zhou Y, Du H, Zhou G. 2021. Rhizome extension
592 characteristics, structure and carbon storage relationships with culms in a 10-year
593 moso bamboo reforestation period. *For Ecol Manag.* 498:119556.
- 594 Lin MY, Hsieh IF, Lin PH, Laplace S, Ohashi M, Chen TH, Kume T. 2017. Moso
595 bamboo (*Phyllostachys pubescens*) forests as a significant carbon sink? A case study
596 based on 4-year measurements in central Taiwan. *Ecol Res.* 32:845–857.
- 597 Liu J, Yang QP, Song QN, Yu DK, Yang GY, Qi HY, Shi JM. 2013. Strategy of fine
598 root expansion of *Phyllostachys pubescens* population into evergreen broadleaved
599 forest. *Chin J Plant Ecol.* 37:230–238.
- 600 Maruo K. 1962. Ecology of moso bamboo species (1) – Growing process of bamboo
601 sprouts. *Bull Tokushima Pref For Exp Stn.* 6:31–33. Japanese.
- 602 Murakami K, Takeuchi I, Teraoka Y. 2006. The above-ground biomass of bamboo
603 *Phyllostachys pubescens* stands in Kagoshima. *Kyusyu J For Res.* 59:121–124.
604 Japanese.
- 605 Nonaka S. 1979. On the vertical distribution of rhizome in a *Phyllostachys pubescens*
606 bamboo stand for bamboo shoot. *Rep Fuji Bamboo Garden.* 31:63–67. Japanese.
- 607 Nonaka S. 1987. Ecology of *Phyllostachys pubescens* rhizome. *Rep Fuji Bamboo*
608 *Garden.* 31:43–51. Japanese.
- 609 Numata M. 1962. Ecology of bamboo forest. *Jpn J Ecol.* 12: 32–40. Japanese.
- 610 Ogawa H. 1977. Principles and methods of estimating primary production in forests. In:
611 Shidei T, Kira T, editors. *Primary productivity of Japanese forests.* Tokyo:
612 University of Tokyo Press. p. 29–35.
- 613 Poorter H, Jagodzinski AM, Ruiz-Peinado R, Kuyah S, Luo Y, Oleksyn J, Usoltsev
614 VA, Buckley TN, Reich PB, Sack L. 2015. How does biomass distribution change
615 with size and differ among species? An analysis for 1200 plant species from five
616 continents. *New Phytol.* 208:736–749.

- 617 R Core Team. 2021. R: A language and environment for statistical computing. R
618 Foundation for Statistical Computing, Vienna, Austria. URL [https://www.R-](https://www.R-project.org/)
619 [project.org/](https://www.R-project.org/).
- 620 Shimono K, Katayama A, Kume T, Enoki T, Chiwa M, Hishi T. 2021. Differences in
621 net primary production allocation and nitrogen use efficiency between moso bamboo
622 and Japanese cedar forests along a slope. *J For Res.* 1–8.
- 623 Song QN, Lu H, Liu J, Yang J, Yang GY, Yang QP. 2017. Accessing the impacts of
624 bamboo expansion on NPP and N cycling in evergreen broadleaved forest in
625 subtropical china. *Sci Rep.* 7:40383.
- 626 Song X, Peng C, Ciais P, Li Q, Xiang W, Xiao W, Zhou G, Deng L. 2020. Nitrogen
627 addition increased CO₂ uptake more than non-CO₂ greenhouse gases emissions in a
628 moso bamboo forest. *Sci Adv.* 6:eaaw5790.
- 629 Sun J, Fan R, Niklas KJ, Zhong Q, Yang F, Li M, Chen X, Sun M, Cheng D. 2017.
630 “diminishing returns” in the scaling of leaf area vs. dry mass in Wuyi Mountain
631 bamboos, Southeast China. *Am J bot.* 104:993–998.
- 632 Suzuki T. 1976. Productivity of moso bamboo (*Phyllostachys edulis*) stands. *Trans Jpn*
633 *For Soc.* 87:223–224. Japanese.
- 634 Suzuki S. 1978. Index to Japanese Bambusaceae. Tokyo: Gakken.
- 635 Takeuchi Y. 1932. Study of bamboo species. Tokyo: Yokendo press. Japanese.
- 636 Tang X, Fan S, Qi L, Guan F, Cai C, Du M. 2015a. Soil respiration and carbon balance
637 in a Moso bamboo (*Phyllostachys heterocycla* (carr.) Mitford cv. *Pubescens*) forest in
638 subtropical china. *iForest.* 8:606–614.
- 639 Tang X, Fan S, Qi L, Guan F, Liu G, Du M. 2015b. Effects of understory removal on
640 root production, turnover and total belowground carbon allocation in Moso bamboo
641 forests. *iForest.* 9:187–194.

- 642 Tang X, Fan S, Qi L, Guan F, Du M, Zhang H. 2016. Soil respiration and net ecosystem
643 production in relation to intensive management in Moso bamboo forests. *Catena*.
644 137:219–228.
- 645 Ueda K. 1960. Studies on the physiology of bamboo with reference to practical
646 application. *Bull Kyoto Univ For*. 30:1–167.
- 647 Umemura M, Takenaka C. 2014. Biological cycle of silicon in moso bamboo
648 (*Phyllostachys pubescens*) forests in central Japan. *Ecol Res*. 29:501–510.
- 649 Utsunomiya T. 1976. Excavation surveys in a moso bamboo stand. *Bull Ehime Pref For*
650 *Exp Stn*. 2:116–121. Japanese.
- 651 Wang X, Liu L, Zhang J, Wang Y, Wen G, Gao R, Gao Y, Zhang R. 2012. Changes of
652 photosynthetic pigment and photosynthetic enzyme activity in stems of *Phyllostachys*
653 *pubescens* during rapid growth stage after shooting. *Chin J Plant Ecol*. 36:456–462.
654 Chinese with English summary.
- 655 Wright IJ, Reich PB, Westoby M, Ackerly DD, Baruch Z, Bongers F, Cavender-Bares
656 J, Chapin T, Cornelissen JHC, Diemer M, et al. 2004. The worldwide leaf economics
657 spectrum. *Nature* 428:821–827.
- 658 Vogt KA, Persson H. 1991. Measuring growth and development of roots. In: Lassoie
659 JP, Hinckley TM, editors. *Techniques and Approaches in forest tree ecophysiology*.
660 Boca Raton FL: CRC Press; p. 477–502.
- 661 Xiao L, Li C, Cai Y, Zhou T, Zhou M, Gao X, Shi Y, Du H, Zhou G, Zhou Y. 2021.
662 Interactions between soil properties and the rhizome-root distribution in a 12-year
663 moso bamboo reforested region: Combining ground-penetrating radar and soil coring
664 in the field. *Sci Total Environ*. 800:149467.
- 665 Yen TM, Lee JS. 2011. Comparing aboveground carbon sequestration between moso
666 bamboo (*Phyllostachys heterocycla*) and china fir (*Cunninghamia lanceolata*) forests
667 based on the allometric model. *For Ecol Manag*. 261:995–1002.

- 668 Yen TM. 2016. Culm height development, biomass accumulation and carbon storage in
669 an initial growth stage for a fast-growing moso bamboo (*Phyllostachys pubescens*).
670 *Bot Stud.* 57:10.
- 671 Yuen JQ, Fung T, Ziegler AD. 2017. Carbon stocks in bamboo ecosystems worldwide:
672 Estimates and uncertainties. *For Ecol Manag.* 393:113–138.
- 673 Zhang F, Wei Y, Akiyama T, Saijoh Y, Kawai H. 2005. Estimating underground
674 biomass of bamboo [*Phyllostachys* sp.] stand using the digital photograph. *J Jpn Agr*
675 *Syst Soc.* 21:65–74. Japanese with English summary.
- 676 Zheng Y, Hong W, Chen L. 1998. Study on structure characteristics of rhizomes in
677 high-yield *Phyllostachys heterocycle* cv. *pubescens* forests. *Sci Silv Sin.* 34:52–59.
678 Chinese with English summary.

679

680

681 **Tables**

682 **Table 1.** Morphology, biomass and net primary productivity (NPP) of the below-ground
 683 rhizomes and roots of a stand of moso bamboo, *Phyllostachys edulis*, at a study site in
 684 western Japan. Rhizome and root data were based on 32 (0.5 m × 0.5 m × 0.5 m) and
 685 18 (cylindrical mesh bags 55 mm in diameter, 0.3 m in length and with 5 mm × 5 mm
 686 mesh size) samples, respectively.

		N	Mean ± standard deviation	Minimum	Maximum
Rhizome	Mean diameter (mm)	32	21 ± 1.7	16	24
	Total node number (m ⁻²)	32	230 ± 120	44	570
	Total length (m m ⁻²)	32	8.4 ± 4.3	2.1	18
	Biomass (g C m ⁻²)	32	810 ± 450	140	1700
	NPP (g C m ⁻² year ⁻¹)	32	90 ± 76	0	290
Root	Biomass (g C m ⁻²)	18	840 ± 280	540	1300
	NPP (g C m ⁻² year ⁻¹)	18	310 ± 240	0	790

688 **Figure legends**

689 **Figure 1** Representative images of the moso bamboo, *Phyllostachys edulis*, stand on
690 Awaji Island, Hyogo Prefecture, western Japan; above-ground standing culms (a) and
691 below-ground rhizome system (b). The excavated area in (b) was 2 m × 2 m. Results
692 from tessellation (solid lines) of three 8 m × 8 m plots based on the spatial distribution
693 of above-ground culms (colored dots) in the bamboo stand (c). As an example, culm
694 position data in 2017 are shown. Dashed lines in (c) indicate failed tessellation.

695

696 **Figure 2** Biomass (a), NPP (b) and turnover rates (c) of various organs of moso bamboo
697 (*Phyllostachys edulis*) on Awaji Island, Hyogo Prefecture, western Japan. Mean and
698 standard deviation values are shown (n = 3 for culms, branches and leaves; n = 18 for
699 roots; n = 32 for rhizomes).

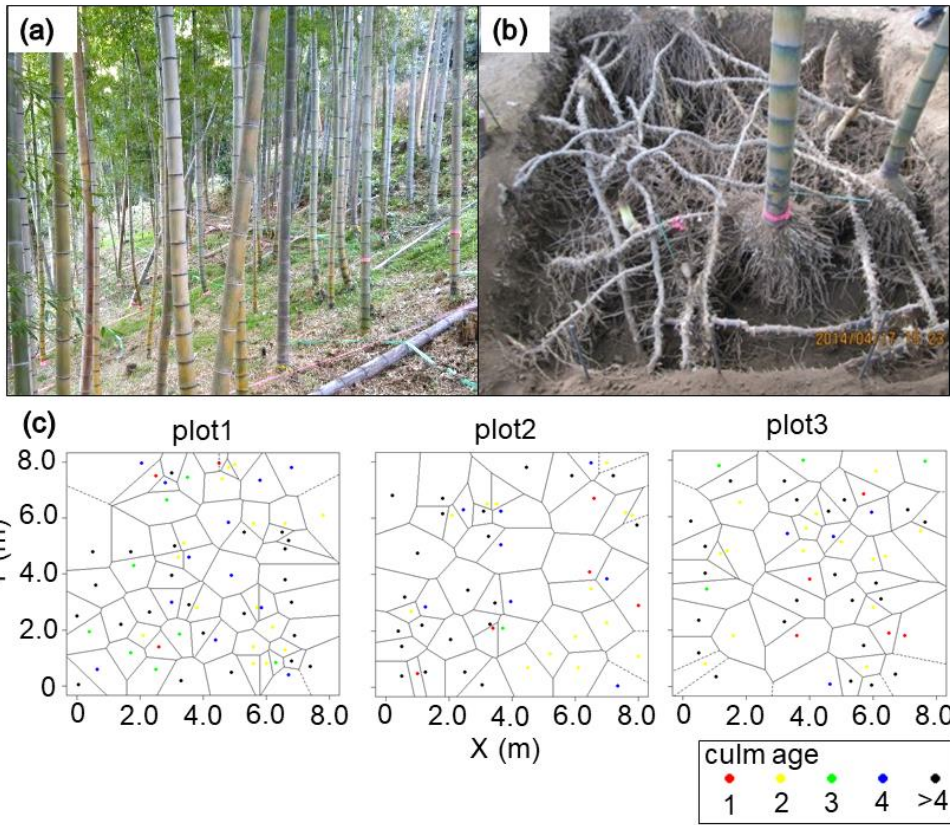
700

701 **Figure 3** Biomass allocation patterns within woody plant individuals and moso bamboo
702 (*Phyllostachys edulis*) ramets at the present study site. Data for woody plants were

703 obtained from Poorter et al. (2015). Biomass allocation to *stems* represents biomass
704 allocated to stems and branches in woody plants, and that allocated to above-ground
705 culms and branches of bamboo. Biomass allocation to *roots* indicates biomass allocated
706 to all below-ground organs (rhizomes, roots and below-ground culm bases of bamboo).
707 To compare these parameters among plants of similar size, woody plant data were
708 filtered for *stems* mass, ranging from 0.66 to 14 kg (n = 842), which is equivalent to the
709 range of moso bamboo measured at the present study site. The dotted lines are isoclines
710 denoting biomass allocation to *leaves* of the ratio; 0, 0.1 and 0.2.

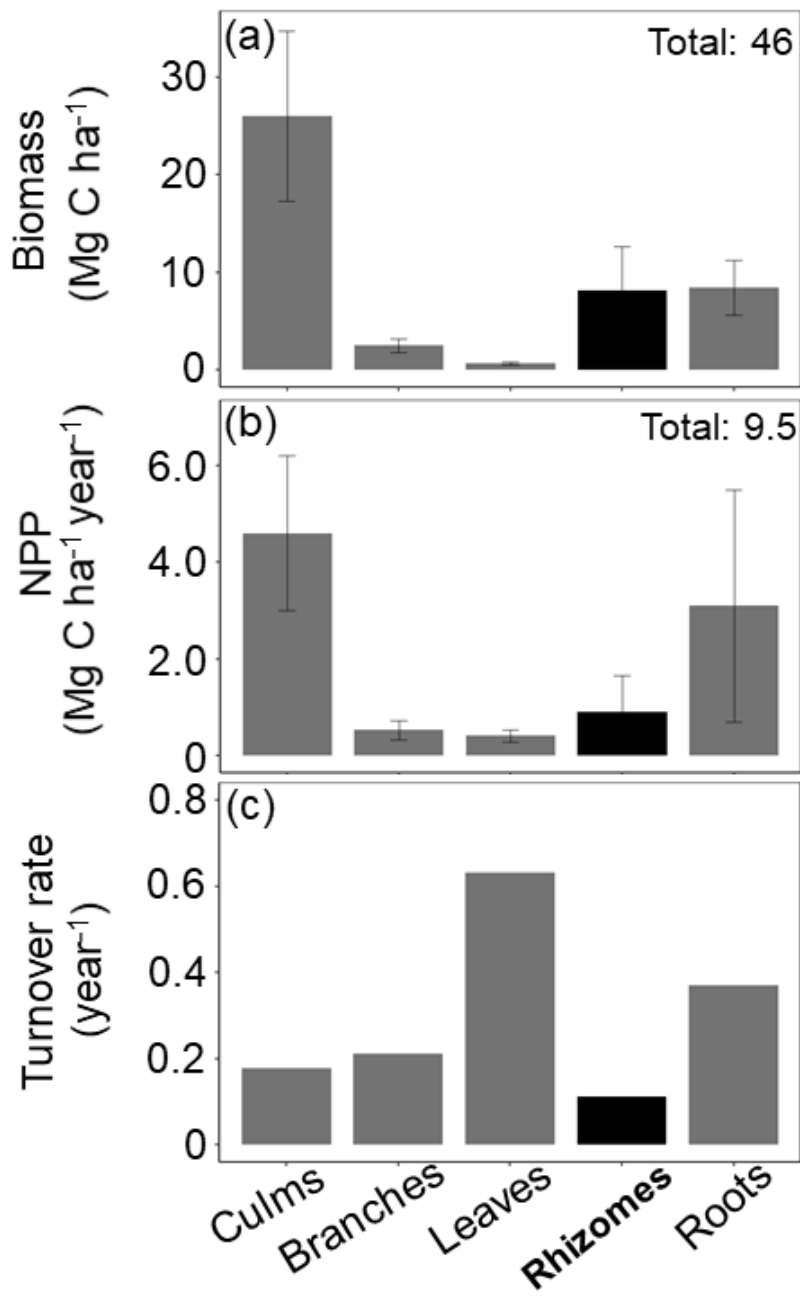
711

712 **Figure 4** The coefficient of variation (CV) of below-ground characteristics, surveyed
713 through excavation with an air spade, plotted against plot size (0.25 m², n = 32; 1.0 m²,
714 n = 8; 4.0 m², n = 2): (a) total number of nodes on rhizomes, (b) rhizome diameter, (c)
715 total rhizome length, (d) rhizome biomass, (e) net primary production of rhizomes;
716 rhizome NPP and (f) root biomass.



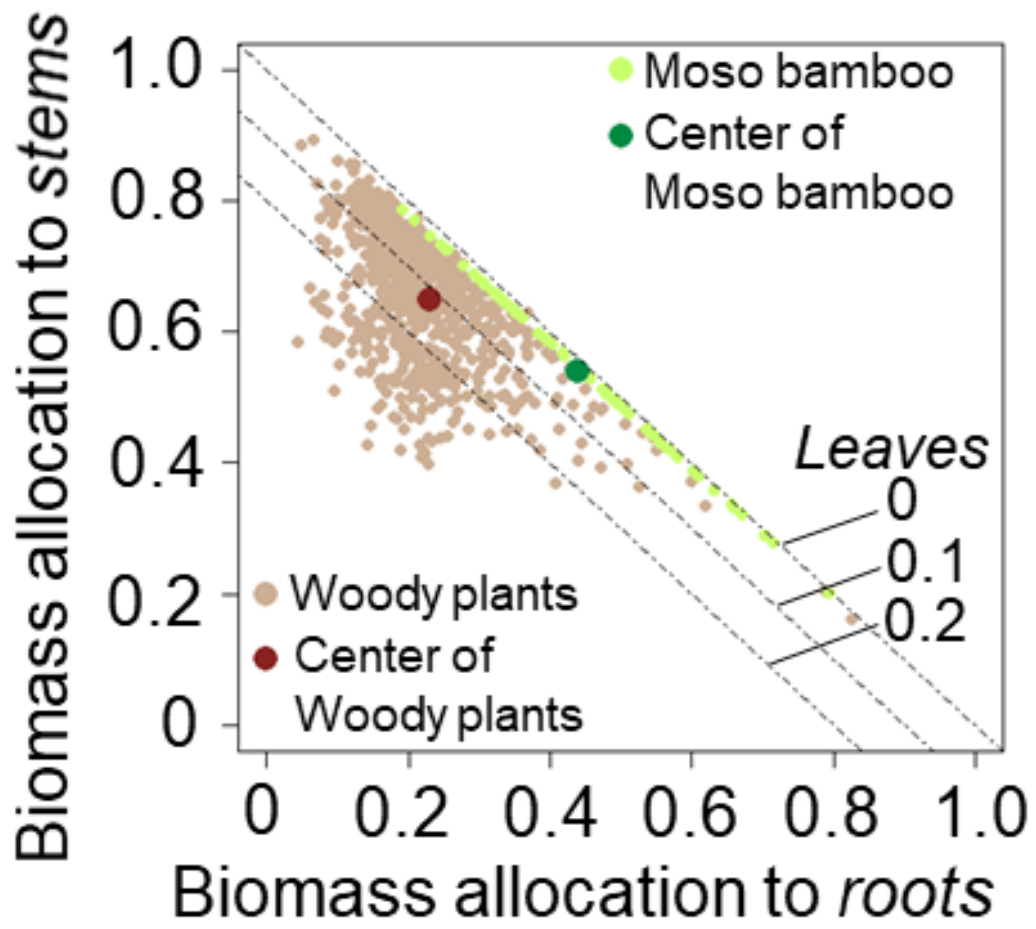
717

718 Fig. 1



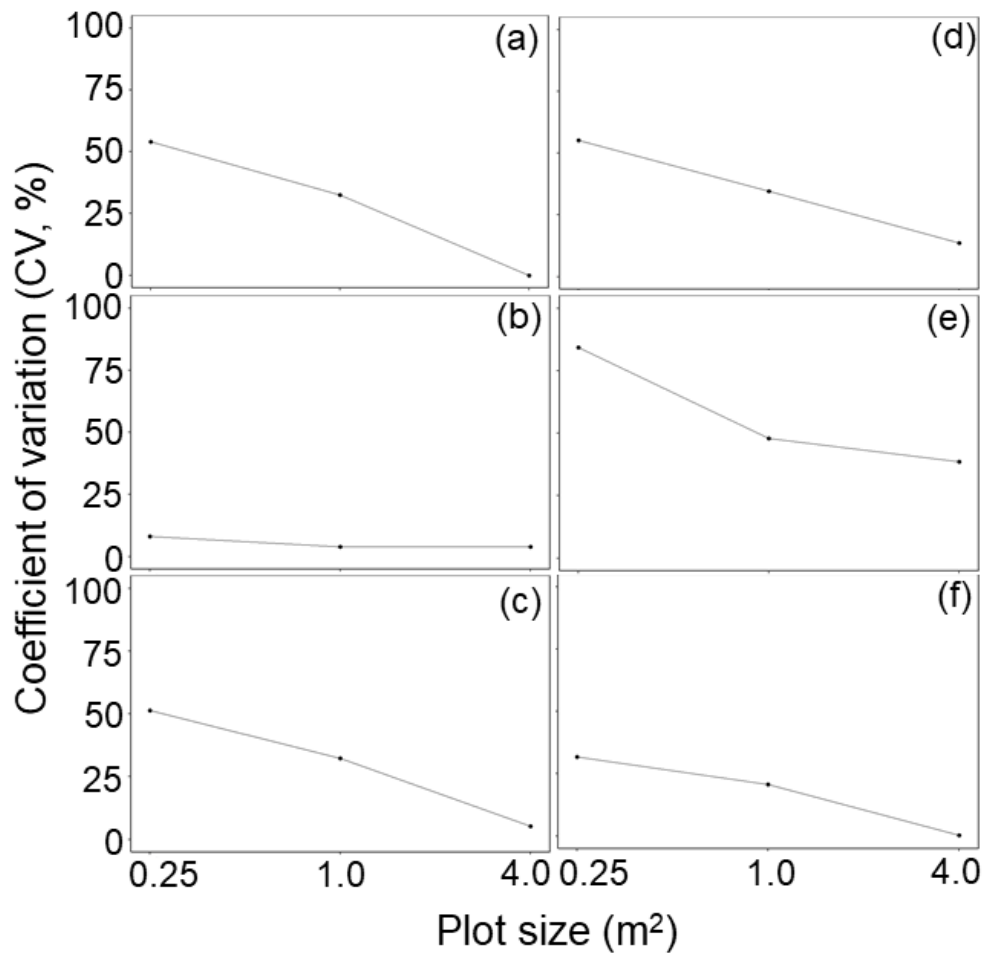
719

720 Fig. 2



721

722 Fig. 3



723

724 Fig. 4

725 **Supplementary materials**

726 **Table S1** Carbon concentrations in organs (leaves, branches, culms, rhizomes, below-ground culm bases and roots) of *Phyllostachys*

727 *edulis* (syn. *P. pubescens*) reported by Fukushima et al. (2015).

Organ	Culm age class	Carbon concentration (g g ⁻¹)
Leaves	one year	0.419
	> one year	0.432
Branches	one year	0.464
	> one year	0.458

Culms	one year	0.463
	> one year	0.468
Rhizomes and below-ground culm bases ^{*1}		0.443
Roots ^{*2}		0.437

728 *1. Below-ground culm base was referred to as the stump in Fukushima et al. (2015).

729 *2. Carbon concentration of roots is the average value for fine and coarse roots from Fukushima et al. (2015).

730 **Table S2** Coefficients of allometric equations ($W_{ij} = \alpha DBH^\beta$) used for estimating the biomass (W_{ij}) of each organ from culm diameter at
 731 breast height (DBH) in moso bamboo, *Phyllostachys edulis*.

Organ (<i>i</i>)	Culm age class (<i>j</i>)	α	β	N	R^2	Reference
Leaves	one year	1.149×10^{-2}	1.515	7	0.853	Abe and Shibata (2009)
	> one year	4.774×10^{-3}	1.976	8	0.851	
Branches	one year	1.045×10^{-1}	1.185	7	0.722	Abe and Shibata (2009)
	> one year	4.647×10^{-2}	1.483	8	0.740	
Culms	one year	6.210×10^{-2}	2.261	7	0.951	Abe and Shibata (2009)
	> one year	1.305×10^{-1}	2.052	8	0.912	

Below-ground culm bases ^{*1}	7.71×10^{-2}	1.434	–	0.954	Fukushima et al. (2015)
Culms > one year	9.7×10^{-2}	2.049	9	0.943	Kaku et al. (2014)

732

*1. Below-ground culm base was referred to as the stump in Fukushima et al. (2015).

733 **Table S3** Interannual variation of net primary production (NPP, Mg C ha⁻¹ year⁻¹) in a stand of moso bamboo, *Phyllostachys edulis*, on
734 Awaji Island, Hyogo Prefecture, western Japan. NPP is shown for each organ: leaves (Leaf NPP), branches (Branch NPP), above-
735 ground culms (Culm NPP) and below-ground culm bases (Culm base NPP) from 2013 to 2017. Mean and standard deviation values are
736 shown (8 m × 8 m plots, n = 3). Note that leaf NPP at stand level was roughly calculated from the leaf biomass and leaf lifespan with
737 consideration of culm ages (see Method for detail).

(Mg C ha ⁻¹ year ⁻¹)	2013–2014	2014–2015	2015–2016	2016–2017	Average
Leaf NPP	–	–	–	–	0.41 ± 0.13
Branch NPP	0.70 ± 0.48	0.22 ± 0.16	0.96 ± 0.07	0.25 ± 0.091	0.53 ± 0.20
Culm NPP	4.4 ± 3.2	2.4 ± 1.8	5.9 ± 0.92	3.3 ± 0.56	4.0 ± 1.6

Culm base NPP	0.85 ± 0.60	0.24 ± 0.18	1.1 ± 0.10	0.29 ± 0.11	0.63 ± 0.25
---------------	-----------------	-----------------	----------------	-----------------	-----------------

739 **Table S4** Morphological characteristics of rhizomes collected during two excavations (2014 and 2018) of a stand of moso bamboo,
 740 *Phyllostachys edulis*, on Awaji Island, Hyogo Prefecture, western Japan. Mean and standard deviation values are shown (0.5 m × 0.5 m
 741 plots, n = 32).

		Mean ± standard deviation	Minimum	Maximum
Mean diameter (mm)	April 2014	21 ± 1.7	16	24
	April 2018	21 ± 3.1	14	26
Total number of nodes of rhizomes (m ⁻²)	April 2014	230 ± 120	44	572
	April 2018	80 ± 70	0	360
Number of rhizome segments (m ⁻²)	April 2014	22 ± 9.8	4	44

	April 2018	8.6 ± 5.9	0	28
Total length (m m^{-2})	April 2014	8.4 ± 4.3	2.1	18
	April 2018	3.7 ± 2.9	0	11

743 **Table S5** Summary of morphological and growth characteristics of moso bamboo (*Phyllostachys edulis*) rhizomes in Japan obtained
 744 from the literature. Mean values are shown. Parentheses indicate range.

RF	Prefecture	Year	Diameter	Internode length	Living bud density		Total length		Annual growth rate		Number	
			cm	cm	m ²	m ⁻¹	m m ⁻²	m system ⁻¹ *1	m year ⁻¹	m ² year ⁻¹	m ²	system ⁻¹
1	-	-	1.6	-	-	-	3.3-11.0	-	-	-	-	-
		1952-1960	2.6	5.3	-	-	2.5-11.3	-	-	-	-	-
			1.7	3.3	-	-						
2	Kyoto	1954	2.1	3.9	-	-	0.8	-	1.68	6.2	0.29	18
			2.2	3.8	-	-	1.1	-	1.84	4.8	0.52	25
		1949-1953	1.2-2.0	-	-	-	1.5	28.4	1.93	-	1.21	23

3	Tokushima	1960–1961	2.0–2.5	3.8–5.9	–	–	7.9–12.0	–	–	–	–	–
4	Ehime	1975	2.2	4.0	29.3	20.1	1.5	112.2	1.29	19.3	1.17	90
5	Fukuoka	–	2.4–2.6	–	–	–	–	–	–	–	4.3 (3.6– 5.2)	–
6	Kumamoto	1985	–	–	–	6.7	–	14.5	1.81 (1.1- 2.65)	–	–	–
7	Gifu	2002–2003	–	(0.20–8.2)	–	–	–	–	1.27 (0.02-3.6)	–	–	–
8	Gifu	2005	–	–	–	–	–	–	1.92 (0.18- 5.50)	–	–	–

9	Osaka	2003	-	-	-	18.6	-	-	2.7 (1.0-5.0)	-	-	-
10	Hyogo	2014	2.1 (1.6-2.4)	-	230 (44-574)* ²	-	8.4 (2.1-18.0)	-	-	-	22 (4-44)	-
		2018	2.1 (1.4-2.6)	-	80 (0-360)* ²	-	3.8 (0-360)	-	-	-	8.6 (0-28)	-

745 RF: Reference, [1] Takeuchi 1932, [2] Ueda 1960, [3] Maruo 1962, [4] Utsunomiya 1976, [5] Nonaka 1979, [6] Nonaka 1987, [7]

746 Kawai et al. 2008, [8] Kawai et al. 2010, [9] Ito and Yamada 2005, [10] This study

747 *1. The unit "system" indicates a connecting rhizome system.

748 *2. Value is "total node density", not "living bud density".

749

750 **Table S6** Summary of above- and below-ground biomass of moso bamboo (*Phyllostachys edulis*) stands in Japan. Studies considering
 751 both above- and below-ground rhizome biomass are included here.

	Culm density (culms ha ⁻¹)	Culm DBH (cm)	Above-ground biomass (Mg C ha ⁻¹)				Below-ground biomass				Total	Below/Above	Rhizome/Total	Rhizome/Below
			Culms	Branches	Leaves	Total	Roots	Rhizomes	Culm bases	Total				
Suzuki (1976) ^{*1,2}	4,500	8.3	19.0	3.3	1.3	23.7	7.7	4.5	–	12.2	35.9	0.52	0.12	0.37
	5,100	9.3	23.0	4.2	1.8	29.1	10.7	6.2	–	16.9	46.0	0.58	0.14	0.37
	8,800	9.2	41.0	5.7	2.4	49.1	9.5	5.9	–	15.4	64.5	0.31	0.09	0.38
Umemura and Takenaka (2014) ^{*1}	2,660	8.2	12.4	1.7	0.6	14.6	11.4	4.4	–	15.7	30.4	1.08	0.14	0.28
	2,400	10.1	17.5	2.1	0.7	20.3	14.4	10.9	–	25.2	45.5	1.24	0.24	0.43
	4,790	11.2	43.1	5.0	1.8	49.9	18.0	11.6	–	29.6	79.5	0.59	0.15	0.39
Isagi et al. (1997)	7,100	11.3	55.5	7.5	2.7	65.7	11.2	7.5	–	18.7	84.4	0.28	0.09	0.40

Fukushima et al. (2015)	9,675	10.5	75.9	6.9	2.1	84.9	27.8	18.2	9.9	55.9	140.8	0.66	0.13	0.33
Goto et al. (2008)	8,200	7.5	31.6	8.1		39.7	19.8	13.0	12.6	45.4	85.1	1.14	0.15	0.29
	8,125	5.4	17.2	3.3		20.5	23.9	15.7	5.1	44.7	65.2	2.18	0.24	0.35
	7,575	8.2	18.0	4.6		22.6	11.8	14.0	8.3	34.1	56.7	1.51	0.25	0.41
Zhang et al. (2005) ^{*3,4}	12,500	4.6	–	–	–	11.1	4.3	7.1	3.4	14.9	25.9	1.34	0.28	0.48
<hr/>														
	6,785 ± 2,983 ^{*5}	8.7 ± 2.1				35.9 ± 22.6				27.4 ± 14.6	63.3 ± 31.7	0.95 ± 0.56	0.17 ± 0.06	0.37 ± 0.06
<hr/>														
This study ^{*1}	7,600	7.6	22	2.5	0.65	25	8.4	8.1	3.5	20	46	0.80	0.18	0.41
<hr/>														
	6,825 ± 2,860 ^{*6}	8.6 ± 2.0				35.1 ± 21.8				26.8 ± 14.1	61.9 ± 30.8	0.94 ± 0.54	0.17 ± 0.06	0.38 ± 0.06
<hr/>														

752 *1. Carbon concentration data reported by Fukushima et al. (2015) were used.

753 *2. Biomass data for the leaf sheath were excluded.

754 *3. *Phyllostachys edulis* - *P. nigra* var. *henonis* mixed stands

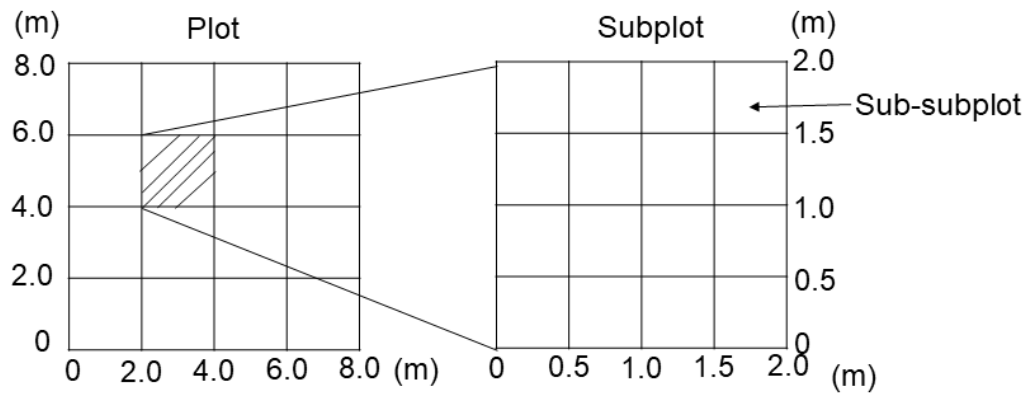
755 *4. No carbon concentration data were available. The values reported by Goto et al. (2008) in the same area were used. Total above-
756 ground C concentration was assumed to be the average value of culm, branch and leaf C concentrations.

757 *5. Mean \pm standard deviation (n = 12)

758 *6. Mean \pm standard deviation (n = 13)

759 **Table S7** Size data used for estimation of below-ground biomass within moso bamboo ramets. The area occupied by each bamboo ramet
 760 (tile area) in three 8 m × 8 m plots was determined based on the spatial distribution of above-ground living culms using Dirichlet
 761 tessellation (an example is shown in Figure 1c). Only closed tiles in 2017 were used for calculation of biomass allocation patterns in
 762 **Figure 3**. The below-ground biomass of each ramet was calculated from the tile area and excavation data, summarized in Table 1 (2014
 763 for rhizomes and 2019 for roots).

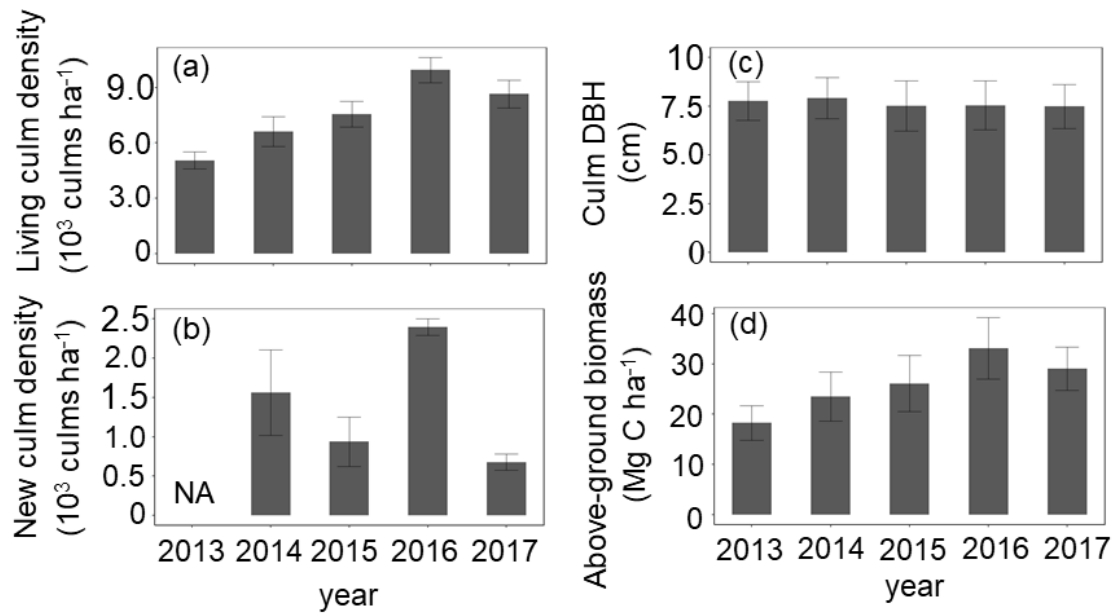
Year	2013	2014	2015	2016	2017
No. total living culms	97	127	145	191	165
No. closed tiles	38	62	70	105	86
Mean tile area (m ²)	2.0	1.5	1.3	1.0	1.2
(Minimum–Maximum)	(1.1–3.5)	(0.44–3.7)	(0.44–3.4)	(0.26–2.3)	(0.26–3.0)



765

766 **Figure S1** Conceptual diagram of a plot at the study site. Each above-ground plot (8 m
 767 × 8 m, see Figure 1) was divided into 16 subplots (2 m × 2 m), and two subplots were
 768 randomly selected for excavation of below-ground rhizomes. Each subplot was divided
 769 into 16 sub-subplots (0.5 m × 0.5 m) for rhizome measurement.

770



771

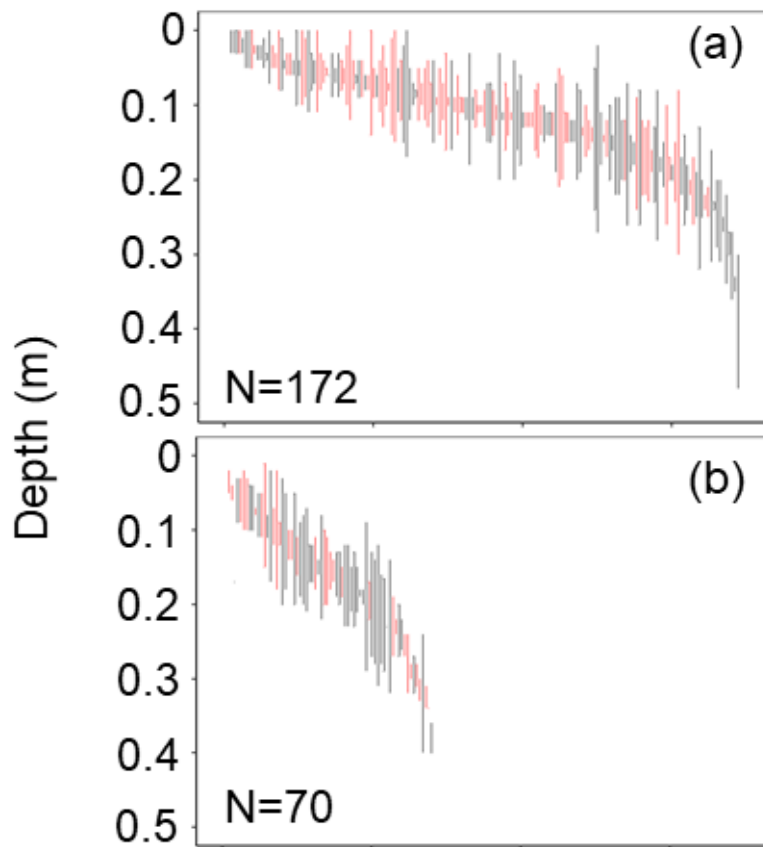
772 **Figure S2** Living culm density (a), newly produced culm density (b), culm diameter at

773 breast height (DBH) (c), and above-ground biomass (d) in the studied moso bamboo

774 (*Phyllostachys edulis*) stand on Awaji Island, Hyogo Prefecture, western Japan. Mean

775 and standard error values are shown (8 m × 8 m plots, n = 3).

776



777

778 **Figure S3** Vertical distributions of below-ground rhizomes in (a) 2014 and (b) 2018 in
 779 the studied moso bamboo (*Phyllostachys edulis*) stand on Awaji Island, Hyogo
 780 Prefecture, western Japan. The shallowest and deepest depth of each rhizome fragment
 781 in each of the 32 sub-subplots (0.5 m × 0.5 m) are shown (N = 172 for 2014 and N = 70
 782 for 2018). Data are arranged in ascending order of average distance from the surface.
 783 Different colors indicate data originating from the two different subplots (2 m × 2 m).

784